# Experimental Study and Parameterization of Interfacial Gas Absorption

Experiments of simultaneous absorption of carbon dioxide and helium, in transient absorption regimes, have been carried out in a gas-liquid flume for stratified-type cocurrent flows. There was a need to improve a method of chromatographic analysis for helium and $CO_2$ titrations in the gaseous phase and the liquid phase; this led us to study simultaneous absorption of $CO_2$ and He independent of dynamic conditions. In addition the dominant wave characteristics were studied and the interfacial friction velocity was measured. It was confirmed that, for two gases presenting a large contrast in diffusivities, gas absorption rates are related directly to the physical properties of the gases. The mass transfer coefficient varies with the $-1/2$ exponent of the Schmidt number for a large interfacial stress and a clean interface whereas it varies with the $-2/3$ exponent for weaker winds.

**B. Caussade**
**J. George**
**L. Masbernat**
Institut de Mécanique des Fluides
Unité de Recherche Associée au CNRS
Avenue du Professeur Camille Soula
31400 Toulouse, France

## Introduction

The interaction mechanisms occurring at a gas-liquid interface under capillary and gravity wave deformation are still misunderstood. This is particularly true concerning turbulence generation inside the liquid phase, close to the interface, where the respective effects of the mean shear stress and the wave-current interactions are not well parameterized.

Hence, one should not be surprised at the lack of success in correctly predicting the absorption rate. This paper presents a new method for studying the absorption of a weakly soluble gas (where the resistance to penetration occurs in the liquid phase).

A great amount of theoretical studies have been carried out: first by Whitman (1923) and Higbie (1935); subsequently by Danckwerts (1951), Levich (1962), Lamont and Scott (1970), Fortescue and Pearson (1967); and more recently by McCready and Hanratty (1984) Kitaïgorodskii (1984), and Back and McCready (1988). The focus of their research differs from one another: small turbulent eddies (Lamont and Scott, 1970; Aïsa et al., 1981); capillary waves (Coantic, 1986); the interfacial diffusive film (Ledwell, 1984; Kitaïgorodskii, 1984); and large interfacial eddies (Fortescue and Pearson, 1967). However, each describes the dynamic state of the interface ("clean" or "dirty," wave slope, wave breaking, turbulence, etc.) with a mass transfer coefficient $K_L$.

The relation of $K_L$ to fluid physical properties and parameters characterizing turbulence or interfacial deformation is still misunderstood.

As shown in Figure 1, the interfacial liquid friction velocity $u_{SL} = \sqrt{\tau_{SL}/\rho_L}$ is correlated well with the absorption coefficient $K_L$, but the significant dispersion of the experimental results shows that other characteristic dynamic scalings are important.

The physical properties of the tracer also play a fundamental role: they are usually characterized by the Schmidt number, value defined as $Sc = \nu_L/D\mu$. For a solid wall, $K_L$ is proportional to (Yaglom and Kader, 1974; Stewart, 1987)

$$K_L \propto \mathrm{Sc}^{-2/3}$$

at a free gas liquid interface stressed by a wind, most theories predict (Ledwell, 1984; Kitaïgorodskii, 1984; Stewart, 1987; McCready and Hanratty, 1984; Coantic, 1986)

$$K_L \propto \mathrm{Sc}^{-1/2}$$

and for weak winds, it can be seen to vary from (Jähne et al., 1987)

$$K_L \propto \mathrm{Sc}^{-2/3} \text{ to } K_L \propto \mathrm{Sc}^{-1/2}$$

The $Sc$ number exponent varies the choice of the gas absorption model; consequently, its determination permits a better comprehension of the role played by the interface agitation in the mass transfer phenomenon.

In this paper the role played by the molecular diffusivity is

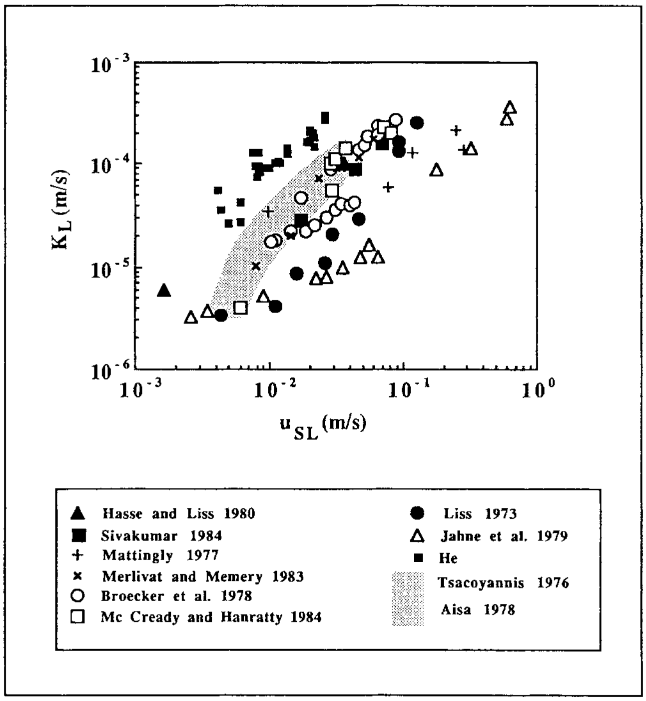

**Figure 1. Mass transfer coefficient $K_L$ vs. interfacial friction velocity $u_{SL}$ in water.**

studied by carrying out simultaneous absorption experiments on two gases with largely different molecular diffusivities. This guarantees that the absorption of the two gases is studied under the same hydrodynamic conditions. It is necessary because changes in the gas mixture affects the shape of the interface by varying the ratio $\rho_L/\rho_G$. Furthermore, the effects of changing the frequency and the amplitude of the dominant wave on $u_{SL}$ are not well known.

Studies were made with carbon dioxide ($CO_2$) and helium (He) even though the helium is not easily analyzed. In fact, it can be noted here that previous experimental failures are mentioned in literature by Merlivat and Memery (1983). The technique used for measuring concentrations in each phase was gas chromatography. The validity of the method is established by comparison with conventional methods of $CO_2$ titration. The results obtained agree with those of Jähne et al. (1987). The liquid-phase resistance is interpreted by velocity-concentration correlations associated with interfacial deformations. These deformations, in turn, are caused by pressure fluctuations associated with two dimensional eddies in the immediate vicinity of the interface.

## Analysis of Schmidt Number

Close to a separation surface, there is a viscous sublayer of constant shear stress, where

$$\tau/\rho_L = \tau_{PL}/\rho_L = u_{SL}^2 = \nu_L \frac{\partial U_L}{\partial z} - \overline{u'w'} = (\nu_L + \nu_T)\frac{\partial J_L}{\partial z} \quad (1)$$

A diffusive layer with a constant mass flux also exists

$$J_s = K_L(C_e - \langle C \rangle) = D_\mu \frac{\partial C}{\partial z} - \overline{c'w'} = (D_\mu + D_T)\frac{\partial C}{\partial z} \quad (2)$$

where the interfacial concentration $C_e$ is determined by Henry's law ($C_e = Hp_i$)

The following dimensionless equations are obtained in the viscous sublayer

$$\frac{\tau P_L}{\rho_L U_{SL}} = 1 = \frac{\partial U^+}{\partial z^+} - \overline{u'w'^+}$$

where

$$U^+ = \frac{U_L}{u_{SL}}, \quad z^+ = \frac{z\, U_{SL}}{\nu}, \quad \overline{u'w'^+} = \frac{\overline{u'w'}}{u_{SL}^2}$$

and

$$\frac{\partial C^{++}}{\partial z^{++}} - \overline{c'w'^{++}} = 1 = \frac{J}{K_L(C_e - \langle C \rangle)}$$

where

$$z^{++} = \frac{z\, K_L}{D_\mu}, \; C^{++} = \frac{C}{C_e - \langle C \rangle}, \; \overline{c'w'^{++}} = \frac{\overline{c'w'}}{K_L(C_e - \langle C \rangle)}$$

Hence,

$$c'^{++} = \frac{c'}{C_e - \langle C \rangle}$$

and

$$w'^{++} = w'/K_L$$

in the diffusive sublayer.

The thickness of the diffusive sublayer can be defined as $\delta_C \propto (D_\mu/K_L)$ and the viscous sublayer is $\delta_\nu \propto (\nu_L/u_{SL})$. There, the ratio of these thicknesses is given as $\delta_C/\delta_\nu \propto [(Sc^{-1} u_{SL})/K_L]$.

According to the results of Aïsa et al. (1981) or Jähne et al. (1987), for example, in the case $Sc = 600$:

$$5.10^{-4} < K_L/u_{SL} < 10^{-2}.$$

Then

$$0.17 < Sc^{-1}\frac{u_{SL}}{K_L} < 3.4$$

In other words, the order of magnitude of the thickness of the diffusive sublayer is same as that of the viscous sublayer. Hence, the region of large interfacial turbulence damping corresponds to the concentration boundary layer.

From the classical point of view, the problem of modeling depends on the determination of the eddy diffusivity

$$D_T^{++} \triangleq -\frac{\overline{c'w'^{++}}}{\dfrac{\partial C^{++}}{\partial z^{++}}} \quad (4)$$

In the immediate vicinity of the interface (Eq. 4) can be written as:

$$D_T^{++} \triangleq -\frac{\overline{c'w'}}{J_S/D_\mu} = k\,z^{++n} \tag{5}$$

where $k$ is a constant and $n$ is an exponent characteristic of the separation surface. In literature, the exponent $n$ is assumed to take the value of 2 at a free interface (Kitaïgorodskii (1984) or Ledwell (1984), which leads to a $-1/2$ Schmidt number dependency for $K_L$. However, experimental results by Baleix (1984) and Jähne et al. (1987) suggest that for weaker winds a $-2/3$ Schmidt number dependency can be reached at a free interface. This behavior is not predicted by theories.

Another approach is to abandon the eddy diffusivity concept and concentrate on the mechanism for generation of velocity concentration fluctuation correlations. From both the momentum equation in the X direction and the diffusion equation, we obtain the equation for $\overline{c'w'}$. When the terms of advective transport are neglected because fully parallel flow is assumed, this may be expressed as follows:

$$\begin{aligned}\frac{\partial}{\partial z^{++}}\left[(1+Sc^{-1})\frac{\partial\overline{w'c'^{++}}}{\partial z^{++}} - Sc^{-1}\overline{w'c'w'^{++}}\right] &= Sc^{-1}\overline{w'^{++2}}\left(\frac{\partial C^{++}}{\partial z^{++}}\right) + Sc^{-1}\,\overline{c'^{++}\frac{\partial^2 w'^{++}}{\partial z^{++}}}\\ &+ \frac{1}{\rho_L K_L^2 Sc}\,\overline{c'^{++}\frac{\partial p'}{\partial z^{++}}} + \overline{w'^{++}\frac{\partial^2 c'^{++}}{\partial z^{++2}}}\\ &+ 2(1+Sc^{-1})\,\overline{\frac{\partial w'^{++}}{\partial z^{++}}\frac{\partial c'^{++}}{\partial z^{++}}}\end{aligned} \tag{6}$$

and when $Sc \gg 1$ we obtain

$$\frac{\partial^2\overline{w'c'^{++}}}{\partial z^{++2}} = \overline{c'^{++}\frac{\partial p'^{++}}{\partial z^{++}}} + \overline{w'^{++}\frac{\partial^2 c'^{++}}{\partial z^{++2}}} + 2\,\overline{\frac{\partial w'^{++}}{\partial z^{++}}\frac{\partial c'^{++}}{\partial z^{++}}} \tag{7}$$

where

$$p'^{++} = \frac{p'}{\rho_L K_L^2 Sc}$$

As shown in Eq. 7, pressure fluctuations are directly related to the creation of $\overline{c'w'^{++}}$, and the presence of waves should greatly increase the order of magnitude of $K_L$.

It follows that at a wall, where $(\partial w'^{++}/\partial z^{++})$ is identically zero, the first nonzero term in Eq. 7 gives $\overline{c'w'^{++}} = 0\ (z^{++3})$, therefore, $K_L \propto Sc^{-2/3}$, and that at a free interface $K_L \propto Sc^{-1/2}$ as $\overline{c'w'^{++}} = 0\ (z^{++2})$. At a free interface without waves, however, the possible nonzero term may be very low and so that Schmidt number dependency varying between $-1/2$ and $-2/3$ could be obtained.

## Molecular Diffusivities of Gases for This Study

### *Molecular diffusivity of $CO_2$*

An analysis of the literature by Baleix (1984) shows that at 25°C the variation of the values of molecular diffusivity of $CO_2$ does not exceed 6%. In Figure 2 a good correlation of the results of three studies [where values of molecular diffusivity, corrected using values of solubilities from the Encyclopédie des Gaz de l'Air Liquide (1976)] are shown and compared with the temperature. The Arrhenius law for temperatures between 0 and 75°C gives

$$D_\mu \times 10^9 = 2{,}359.7 \cdot \exp(-2{,}123/T)\ \mathrm{m^2/s} \tag{8}$$

where $T$ is expressed in Kelvin,

A linear law for temperatures between 0 and 35°C gives

$$D_\mu \times 10^9 = 0.9101 + 0.0405\,\theta\ \mathrm{m^2/s} \tag{9}$$

where $\theta$ is expressed in degrees Celsius.

### *Molecular diffusivity of helium*

A review of the papers written between 1960 and 1980 demonstrates a variation in the measured helium diffusivity molecular values of up to 30% at 25°C provided that out-of-range values are ignored (Boerboom and Kleyn, 1969; Baird and Davidson, 1962). Whenever possible, diffusivities were recalculated using solubilities from Benson and Krause (1976), which are close to those of Weiss (1971). This correction in some cases is very important, and the variation of diffusivities recalculated taking this into account is greatly improved as shown in Figure 3.

All these values, in the range of 10 and 60°C, comply with an Arrhenius-type law

$$D_\mu \times 10^9 = 1{,}625.4 \cdot \exp(-1{,}623/T)\ \mathrm{m^2/s} \tag{10}$$

or a linear law

$$D_\mu \times 10^9 = 0.1787\,\theta + 3.4305\ \mathrm{m^2/s} \tag{11}$$

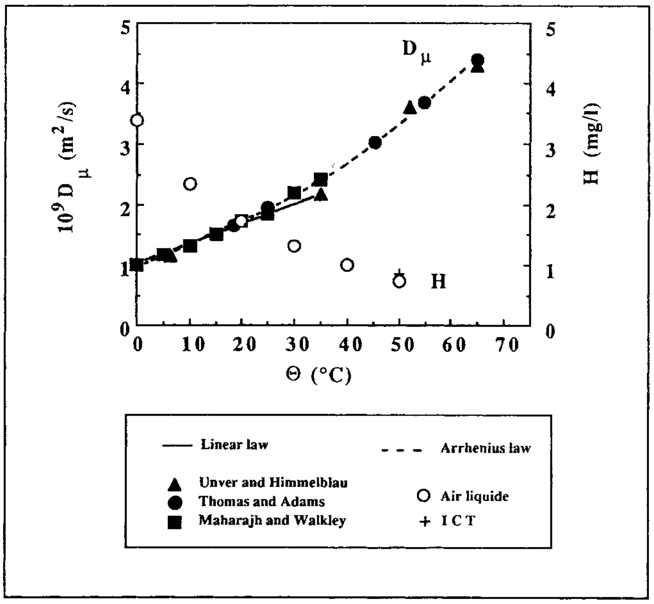

Figure 2. Molecular diffusivity and solubility of $CO_2$ vs. temperature.

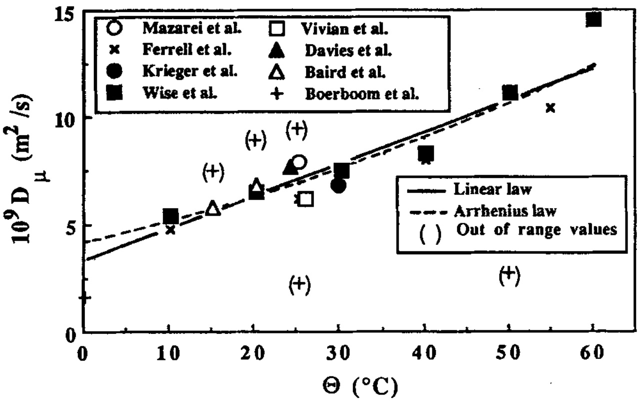

Figure 3. Corrected molecular diffusivity of helium vs. temperature.

In this review of the literature it is shown that the diffusivity value for $CO_2$ is well known and that of He can be accepted when the out-of-range values, compared with the six other studies analyzed, are eliminated.

## Mass Transfer Coefficient

Gas absorption of carbon dioxide and helium has been carried out in a cocurrent parallel gas liquid flow. Here, $J_s$ represents the average gas flow through the air-water interface, $\langle C \rangle$ represents the bulk concentration of dissolved gas in the liquid, and $C_e$ represents the average concentration at the interface itself. The kinetics of interfacial transfer are considered rapid enough to keep $C_e$ in equilibrium with the partial pressure $p_i$ of the gas just above the interface. The mass transfer coefficient is defined by

$$K_L = \frac{J_s}{[C_e(t) - \langle C(t) \rangle]} \tag{12}$$

This supposes that the water concentration is uniform between the test sections.

Mass transfer coefficient $K_L$ is calculated from absorption experiments consisting of a continuous invasion of the gaseous phase and measurement of the concentration time variations in both the inflow $S_1$ and outflow $S_2$ sections in the liquid phase. The gas-phase concentration is measured only in the middle of the gaseous phase since the concentration of the gaseous phase is uniform along the channel.

The flux of gas at the interface is

$$J_s = h_L \frac{d\langle C(t) \rangle}{dt} \tag{13}$$

and according to Eq. 12

$$\frac{d\langle C(t) \rangle}{dt} = \frac{K_L}{h_L}[C_e(t) - \langle C(t) \rangle] \tag{14}$$

If $\Delta T = x/\langle U_L \rangle$ is the average path time of a fluid particle between sections $S_1$ and $S_2$, and the concentration in section $S_1$ at time $t$ is called $\langle C_1 \rangle$ and that in section $S_2$ at time $t + \Delta t$ is called $\langle C_2 \rangle$, by integrating Eq. 14, the following relation is obtained

$$K_L = \frac{h_L[\langle C_2 \rangle(t + \Delta T) - \langle C_1 \rangle(t) \exp(-K_L/h_L)\Delta T)]}{\exp(-(K_L/h_L)\Delta T \int_0^{\Delta T} C_e(t + \tau) \exp[(K_L/h_L)\tau]\, d\tau} \tag{15}$$

When the steady state in tracer concentration is reached, this expression leads to the conventional logarithmic relation

$$K_L = \frac{h_L}{\Delta T} \log\left(1 + \frac{\langle C_2 \rangle - \langle C_1 \rangle}{C_e - \langle C_2 \rangle}\right)$$

An implicit expression of $K_L$ is obtained by Eq. 15, which can be solved iteratively, provided that the $C_e$-time-dependent law is known.

According to Merlivat and Memery (1983)

$$V_G \frac{d_{p_i}}{dt} = P\Phi - p_i \Phi' \tag{16}$$

where $\phi$ is the discharge inflow rate of gas in the gaseous phase and $\phi'$ that leaking outside the flume, provided that the absorbed gas quantity is negligible.

Hence, using Henry's law (Eq. 16) we obtain

$$C_e(t) = a[1\text{-}\exp(-bt)] \tag{17}$$

$a$ and $b$ are computation constants adapted to suit the experimental conditions.

The graphs of Figure 4 fit well with Eq. 17 for $CO_2$ and He, and Eq. 15 gives

$$K_L = \frac{h_L(\langle C_2 \rangle(t + \Delta T) - \langle C_1 \rangle(t) \exp[-(K_L/h_L)\Delta T)]}{a\left\{h_L/K_L - \frac{\exp[-b(t + \Delta T)]}{K_L/h_L - b} + \left[\frac{\exp(-b\Delta T)}{K_L/h_L - b} - h_L/K_L\right] \exp[-(K_L/h_L)\Delta T)]\right\}} \tag{18}$$

## Experimental Method

### *Experimental facilities*

Experiments were carried out on the $C_1$ flume of the IMFT. These facilities provide separated cocurrent gas-liquid flows. The geometry of the channel is such that the flow becomes internal signifying that the wall and interfacial boundary layers are fully developed. The experimental facility (see Figure 5) has the following characteristics:

- The flume is 12 m long, 0.2 m wide and 0.1 m high.

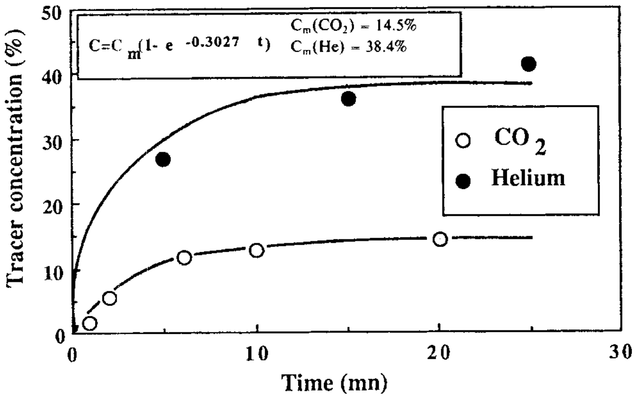

Figure 4. Experimental values and theoretical laws of $CO_2$ and He concentration in the channel.

- The recirculating gas flow is provided by a regulated direct-current powered blower, $0 < Q_G < 0.25\ m^3/s$.
- The recirculating liquid flow is provided by a two-speed centrifugal pump, and a desorption disposal is used, $0 < Q_L < 4$ L/s.
- $Q_G$ is measured with a venturi meter and $Q_L$ with a diaphragm.

Each test section is equipped with:

- A transparent pot linked at its upper section to the gaseous phase and at its lower part to the liquid phase. It allows precise determination of the mean interfacial level as it works as a low-pass filter for interfacial-level fluctuations.
- Optical glass windows on each lateral wall to permit the use of a LDA system for liquid velocity measurements.
- A door on the upper part of the section to insert a hot wire probe in the gaseous phase for gas velocity measurements or capacitance wires for interfacial level recordings.

## *Experimental conditions*

The reservoir is filled up with deionized water to provide pure water, which is needed to study "clean" interfaces and which allows the use of conductimetry as a standard to validate concentrations of $CO_2$ in water. After dynamic stabilization of the flows, gas ($CO_2$, He, or $CO_2$ + He) is injected from storage tanks. The gas flow rate is set to 1 L/s for He and 0.4 L/s for $CO_2$. Liquid samplings are made at sections $S_1$ and $S_2$ for fetches of 0.4 m and 11.55 m, and gaseous samplings in the middle of the channel at 6.25 m.

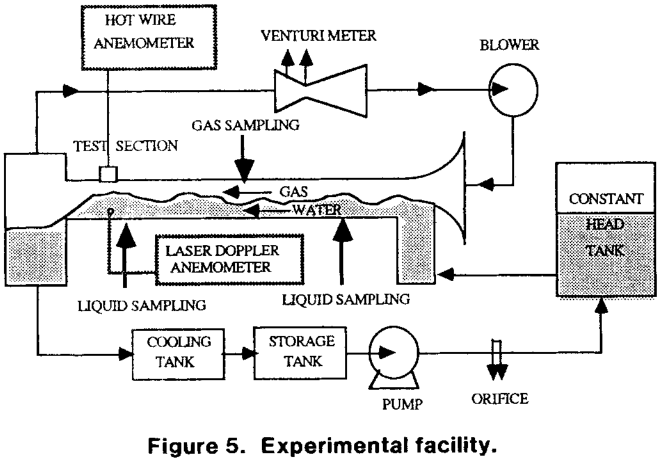

Figure 5. Experimental facility.

## *Determination of dynamic parameters*

High concentrations of gases, varying with time and involving time-dependent dynamic rates make velocity measurements difficult in all phases. Nevertheless, there is a very complete data bank by Suzanne (1985) and Fernandez Flores (1984) for cases where water and air alone coflow. An estimation of the friction velocity $u_{SL}$ characteristic of the interfacial turbulence is obtained by controlling the displacement of the maximum velocity in the gaseous phase by means of a pitot tube and a micromanometer. Mean water levels are directly read on the transparent pots placed along the channel with a cathetometer. Water level fluctuations are measured by means of capacitance probes and recorded on a Euromag (Schlumberger) recorder and processed on a Hewlett Packard spectrum analyzer.

## *Analysis for He and $CO_2$*

Titrations are made by means of gaseous chromatography using a technique, believed to be original, which includes the following steps:

*Sampling and Analyzing of Liquid Concentration.* Liquid samples are poured out of the channel into Pyrex containers equipped with two taps, one at each end. Before isolating the sample, water flows through the container for one to two minutes to be sure that all air is driven out and that the sample is representative of the liquid phase.

The container is connected to the chromatography loop (see Figure 6) when two needles are driven into the elastomer membrane of the container. Water is circulated through the loop by the pump when the valve is in position. (The loop and both needles are filled with distilled water before the membrane is pierced.) When the water to be analyzed has been circulated for 30 minutes (time obtained by experience), it uniformly fills the circuit including the loop. By turning the valve, water in the loop is injected into the chromatograph. As soon as dissolved gases (He, $O_2$, $CO_2$, etc.) are detected, the valve is turned to allow

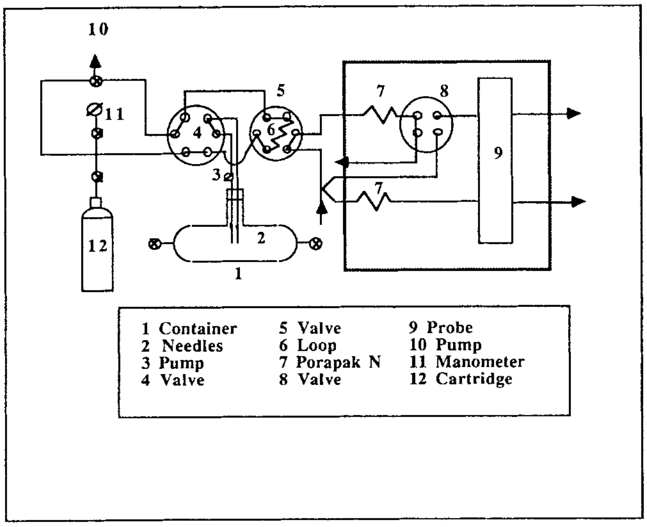

Figure 6. Handling and chromatograph injection fluid circuits.

evacuation of injected water out of the chromatograph preventing it from passing via the thermal conductivity probe.

Utmost care must be taken when measuring volumes (containers, circuits, loop) and the temperature during experiment since they affect the quantitative titration. Analyzing a sample can give significant results, only when air is totally pumped out of the sampling container and the liquid which dissolved the air is replaced by fresh sampling water and there are no helium leaks between sampling and end of titration. It has been found that if titration is carried out within 8 hours, there is no significant loss of helium.

The volume of the circuit including needles is filled up twice with distilled water. Here, the dilution of gas is:

$$\frac{C_{\text{final}}}{C_{\text{initial}}} = \frac{47.76}{47.76 + 2.894} = 0.9429$$

*Sampling and Analyzing of Gas Concentration.* Gaseous samples from the gaseous phase are stored in metal cartridges which are connected to the upper part of the channel once a vacuum has been created. The gaseous sample is drawn out when the cartridge tap is opened. The filled cartridge in Figure 6 is connected to the circuit, and its tap remains closed. A vacuum is created in the circuit by the pump, and the residual air pressure is measured with the manometer. Once vacuum stabilization has been checked, a certain amount of gas to be analyzed is let in through the cartridge tap. After stabilization, when the gas pressure is measured, the sample contained in the loop is injected into the chromatograph through the valve.

*Experimental Standardization.* A cartridge of pure He or pure $CO_2$ is connected to the circuit. It is then processed in the same way as for gaseous titration. Injection of a standard volume (that of loop) under different pressures, at well known temperatures, allows a standardization curve of the chromatographic integration signal to be plotted against the number of gas molecules injected. The standardization curve is plotted for the range of values reached while titrating aqueous or gaseous samples. It is therefore a method for titrating He and $CO_2$ in both fluids.

*Experimental Setup.* A H.P. 5880 gas chromatograph equipped with a one-filament thermal conductivity detector linked to a H.P. 3390 electronic integrator was used. The column was filled with 80–100 mesh Porapak N/7/, 5 m in length and 1/8 in. (3.2 mm) in diameter. The temperature of the column was set to 120° for gas titrations and to 160° for water evacuation. It was programmed to have the temperature range of 40 to 70°C for liquid titrations. The gas vector (nitrogen) discharge was 15 mL/min.

*Validation of the Method.* For He detection, only the chromatography method was used. For $CO_2$, the chromatography results were compared with the standard process described below.

In the gaseous phase, the $CO_2$ was titrated by a Schlumberger Infrared absorber analyzer. In the liquid phase, a conventional electrical conductivity method was used.

In the gaseous phase, as shown in Figure 7, problems were encountered with the programming of temperatures. This was not the case for the 120°C isothermal analyses; this process was therefore adopted. Considering that the standard method of infrared analyses is not error-free, these chromatography and infrared methods validate each other although $CO_2$ concentrations appear to be slightly overestimated by chromatography. In the liquid phase, as shown in Figure 8, the average $CO_2$ chromatography concentration measurements remain 5% below the conductivity measurements. This could be due to difficult integration conditions (inclined ground line, spread out peaks).

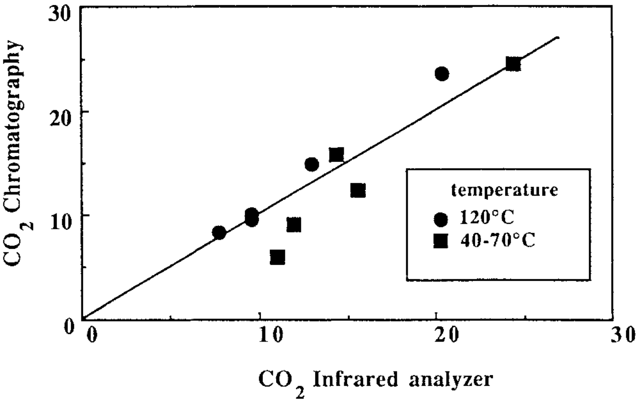

**Figure 7. $CO_2$ concentrations in the gaseous phase.**

Considering these results, this technique seems fairly valid for titrating liquid and gaseous samples. In addition, it allows simultaneous detection of $CO_2$ and He which is absolutely necessary as previously discussed.

## Results and Conclusion

Let us recall that this study is concerned with the characterization of the role played by gas molecular diffusivity in absorption when resistance to penetration is located in the liquid phase.

In the interests of increasing the sensitivity of measurements with regard to the dissolved gas concentrations, high concentration levels of $CO_2$ and especially of He in the gaseous phase were used. As can be seen in Figures 9a and 9b, wave amplitude spectra obtained for different flow rates and for different gas-phase compositions are strongly dependent on these factors (Table 1). In Figures 9a and 9b, we can see that the dominant wave frequency, characterized by big eddies close to the interface, is strongly influenced. This, however, could have only a minor effect on gas absorption. Nevertheless, it appears, from Figure 9a, that for concentrations greater than 40%, the energy at the higher frequencies is also dramatically changed. Hence, the dis-

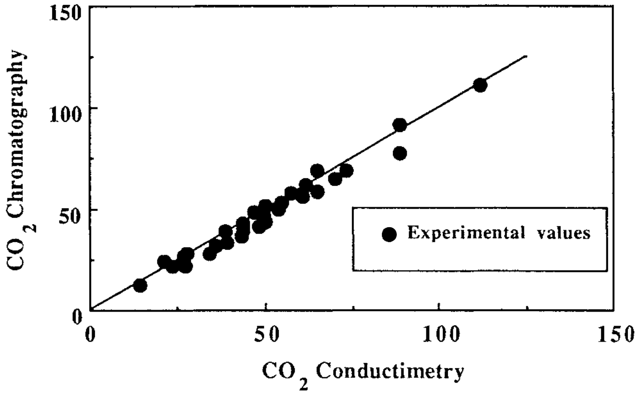

**Figure 8. $CO_2$ concentrations in the liquid flows.**

Table 1. Flow Parameters

| Run | $\langle \overline{U_{1G}} \rangle$ m/s | $\rho_G$ kg/m$^3$ | $u_{SL}$ cm/s | $\lambda\ 10^2$ m | $\sqrt{\overline{h'^2}}$ m | $f_0$ Hz | $C_T$ m/s | $K_w$· |
|---|---|---|---|---|---|---|---|---|
| 1 | 3.92 | 1.232 | 0.71 | 5.5 | 0.97 | 14.2 | 0.79 | — |
|  | 4.02 | 1.43 | 1.14 | 5 | 1 | 15.2 | 0.77 | 1.78 |
|  | 3.32 | 0.38 | 0.45 | — | — | — | — | — |
|  | 3.65 | 0.797 | 0.55 | — | — | — | — | — |
| 2 | 5.8 | 1.227 | 1.82 | 10.8 | 2.55 | 8.8 | 0.957 | — |
|  | 5.98 | 1.389 | 2.01 | 11.7 | 2.02 | 8.4 | 0.979 | 0.71 |
|  | 5.77 | 0.531 | 0.78 | 5.2 | 0.87 | 14.9 | 0.892 | 1.29 |
|  | 5.19 | 0.891 | 1.14 | 10.4 | 1.82 | 8.8 | 1.008 | 1.98 |
| 3 | 8.15 | 1.235 | 2.61 | 28 | 5.13 | 4.7 | 1.31 | — |
|  | 8.26 | 1.3 | 2.57 | 27.5 | 4.8 | 5 | 1.37 | 0.87 |
|  | 7.04 | 0.85 | 2.17 | 14 | 4.66 | 5.6 | 1.04 | 1.44 |
|  | 7.9 | 1.003 | 2.59 | 23 | 5.88 | 5.1 | 1.17 | 1.34 |

tribution of small structures, which is believed to control mass transfer, is also affected. *Therefore, simultaneous He and $CO_2$ absorption experiments were chosen* to characterize the role played by molecular diffusivity alone. All experimental results are summarized in Table 2.

Figure 10 shows the mass transfer coefficient vs. Schmidt number for three different flow velocities. For rather strong winds, $K_L$ is fairly well related to the $-0.5$ Schmidt exponent. This suggests that a mobile interface cannot be considered as a solid wall since this would require a $-2/3$ exponent for the Schmidt number. These results are in good agreement with the dynamic studies by Fabre et al. (1982) and Suzanne (1985) on the same channel, and also by Marodon (1983), Caussade et al. (1982), Souyri (1986), and Moussa (1986) for deeper channels. All these studies show that close to a gas-liquid interface there is no evidence, as in the case of a solid wall, of a high-turbulence production by mean velocity gradient. On the contrary, a high

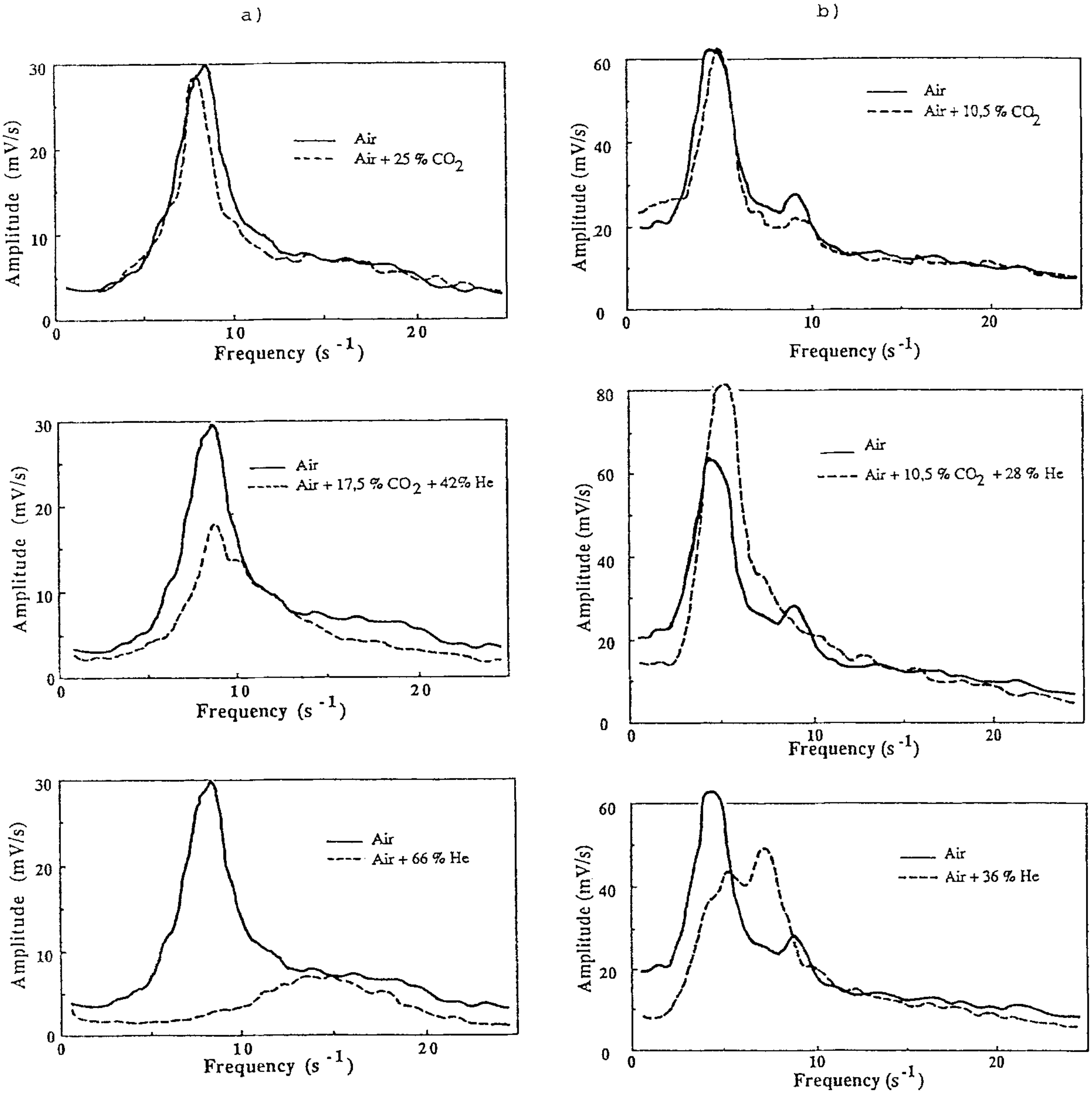

Figure 9. Interface height fluctuation amplitude spectra: a. Run 2; b. Run 3.

Table 2. Absorption Experiments of He and $CO_2$

| | | $CO_2$ | | | | | He | | | |
|---|---|---|---|---|---|---|---|---|---|---|
| | | | | $10^5 K_L$ m/s | | | | | $10^5 K_L$ m/s | |
| $\overline{\langle U_{1G} \rangle}$ m/s | $u_{SL}$ cm/s | $C_m$ % | $Sc$ | Conduct. | Chromato. | Avg. | $C_m$ % | $Sc$ | Chromato. | Avg. |
| 3.76 | 0.566 | 20.6 | 760 | 1.7 | 1.2 | 1.3 | 53.5 | 203 | 2.7 | 3.5 |
| 3.75 | 0.566 | | | 1.4 | 0.9 | | | | | |
| 5.79 | 1.153 | | | 6.9 | 7.2 | | | | 10.3 | |
| 5.78 | 1.118 | 24.5 | 620 | 7.6 | 6.2 | | 38.4 | 166 | 10.1 | |
| 5.78 | 1.114 | | | 7.3 | 6.2 | | | | 10.6 | |
| 5.83 | 0.985 | | | 5.2 | 3.9 | | | | 9.1 | |
| 5.86 | 0.889 | 14.5 | 740 | 5.7 | 4.4 | 5.9 | 38.2 | 198 | 9.7 | 11 |
| 5.86 | 0.883 | | | 5.9 | 5.5 | | | | 9.6 | |
| 5.89 | 1.338 | | | 5.5 | 3.9 | | | | 13.8 | |
| 5.9 | 1.334 | 16 | 688 | 5.8 | 6.1 | | 27 | 184 | 12.6 | |
| 5.9 | 1.338 | | | 6.9 | 6.8 | | | | 13.3 | |
| 8.72 | 2.608 | | | 11.6 | 15.3 | | | | 28.8 | |
| 8.72 | 2.600 | 9.5 | 792 | 13.5 | 14.2 | 13.9 | 23.4 | 212 | 27.5 | 27.8 |
| 8.72 | 2.600 | | | 14.6 | 14.2 | | | | 27 | |

level of kinetic energy diffusion by pressure fluctuation redistribution and nonisotropic velocity fluctuation destruction can be seen.

For lower gas velocities, however, the two-dimensional interfacial turbulence does not impose pressure-concentration fluctuation correlations and the interface remains smooth (as predicted by Gastel for lower liquid friction velocities). Therefore, the interface behaves closer to a wall for mass transfer and $K_L$ is related to the $-2/3$ Schmidt number exponent.

Although dynamic flow parameters are difficult to measure in the presence of high $CO_2$ or He gas concentrations, the interfacial friction velocity $u_{SL}$ was estimated using average gas concentration levels. $K_L$ vs. $u_{SL}$ remains for $CO_2$ in the range of results previously obtained for $CO_2$ in our laboratory. However, as shown in Figure 1, the results for He are clearly higher. They confirm that absorption experiments with continuous invasion of tracers give results which are comparable to those for a steady-state case and that high absorption levels are directly related to high molecular diffusivity values.

The prediction of the mass transfer coefficient seems to be mainly concerned with the determination of characteristic interfacial scalings. As $K_L\sqrt{Sc}/u_{SL}$ ranges between 0.05 and 0.2, it appears that the friction velocity is not the only parameter representative of the interfacial agitation. For this reason, the model proposed by Coantic (1986) that relates mass transfer to the shape of capillarity waves and hence to the small interfacial eddies seems attractive:

$$K_L \propto u_{SL}\, \alpha'^{1/2}\, Sc^{-1/2}$$

where

$$\alpha' \propto -\overline{\left(u' \frac{\partial^2 u'}{\partial x\, \partial z}\right)}$$

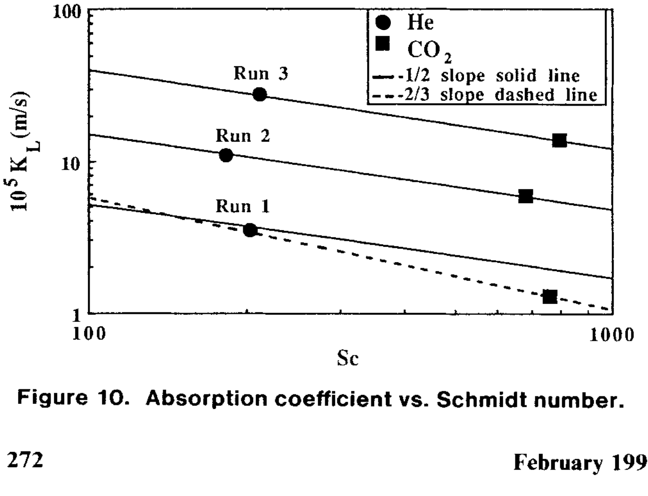

**Figure 10. Absorption coefficient vs. Schmidt number.**

Unfortunately, in this modeling $\alpha'$ is related to a power of $u_{SL}$ which is not the only parameter characterizing the vertical agitation of the interface.

The explanation of the results could be associated with understanding the turbulent kinetic energy in the liquid close to the interface. As was shown by Suzanne (1985) and Kitaïgorodskii et al. (1983), close to the interface the classical wall correlation between turbulent kinetic energy and friction velocity is not valid. Below the waves, the non-dimensional value of 7.5 for $e/u_{PL}^2$ is not reached, in fact, there is a variation of $e/u_{SL}^2$ up to 30 and above for larger fetches. Again for a large range of absorption experiments (Figure 11) carried out for various types of lows in the IMFT [George (1987) for counter-current film and also deep channel with developing fetches, large two-dimensional waves ($h'^2 \simeq 0.02$ m) and no liquid flow rate] with interfacial shape being controlled essentially by gas-phase turbulence or by liquid wall turbulence, $K_L$ could be better related to the turbulent kinetic energy below the waves, $e$, than to $u_{SL}$.

This turbulent kinetic energy, $e$, can be assumed as being related to the dominant wave energy. As shown on Figure 12, $K_L Sc^n/u_{SL}$ appears to be clearly related to a nondimensional dominant wave energy ($K_w^+ = f^2\, h'^2/u_{SL}^2$) capable of fitting results as different as those obtained for the present study and for a developing fetch. The correlation is given approximately by

$$\frac{K_L Sc^n}{u_{SL}} = 0.13\sqrt{K_w^+}$$

## Acknowledgment

The authors would like to express thanks to Professors J. Mathieu and L. Torres, Analytical Chemistry Laboratory of the E.N.S.C.T., the Institut

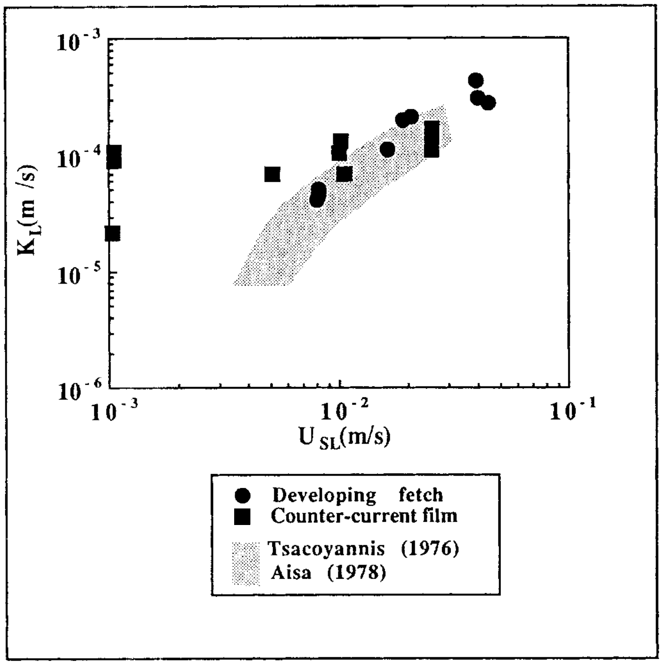

**Figure 11. Absorption coefficient under different interfacial turbulence conditions.**

National Polytechnique de Toulouse for their assistance in making this research possible. The technical support of F. Cometto of the Institut de Mécanique des Fluides de Toulouse is also appreciated.

## Notation

$A,a,b$ = constants
$C_e$ = equilibrium concentration
$C_m$ = average gas-phase concentration of tracer
$c'$ = local concentration fluctuation in the liquid phase
$\langle C_i \rangle$ = average dissolved gas concentration in the liquid phase in section $i$
$C_T$ = dominant wave celerity
$D_\mu$ = molecular diffusivity
$D_t$ = eddy diffusivity
$e$ = turbulent kinetic energy
$f_0$ = dominant wave frequency
$Fr$ = Froude number = $(u_{SL}^2/g \cdot h_L)(\rho_L \rho_G)$
$g$ = gravity constant
$H$ = Henry's law constant
$h_L$ = liquid depth

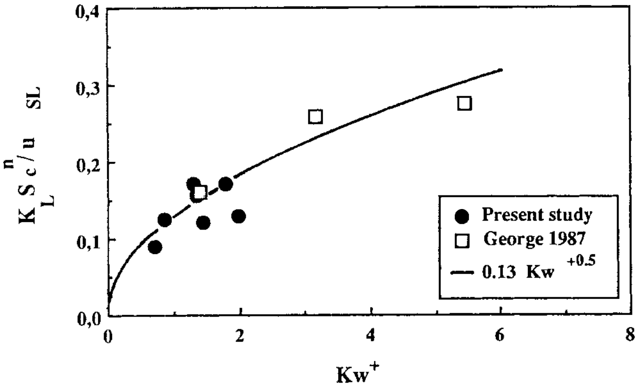

**Figure 12. $K_L Sc^n/u_{SL}$ vs. nondimensional dominant wave energy $K_w^+$.**

$h'$ = interface height fluctuations
$J_s$ = interfacial mass flux
$K_L$ = mass transfer coefficient
$P$ = total pressure
$P_i$ = partial pressure in the gas phase
$Q_G$ = gas phase flowrate
$S$ = interfacial area
$S_i$ = test section $i$
$Sc$ = Schmidt number = $D_\mu/\nu_L$
$T$ = temperature, K
$t$ = time
$U_G$ = average velocity in the gas phase
$U_L$ = average velocity in the liquid phase
$u_{PL}$ = wall friction velocity
$u_{SG}$ = interfacial gas friction velocity
$u_{SL}$ = interfacial liquid friction velocity
$u'$ = streamwise velocity fluctuation
$w'$ = transverse velocity fluctuation
$v_G$ = channel gas volume
$x$ = streamwise coordinate
$z$ = vertical coordinate
$\Delta T$ = time lag

### *Greek letters*

$\alpha$ = coefficient
$\gamma$ = electrical conductivity of the liquid
$\theta$ = temperature, °C
$\lambda$ = dominant wave length
$\nu_L$ = kinematic viscosity of the liquid
$\nu_t$ = eddy viscosity of the liquid
$\rho_G$ = gas density
$\rho_L$ = liquid density
$\tau$ = time
$\tau_{PL}$ = liquid wall shear stress
$\tau_{SL}$ = interfacial shear stress
$\phi$ = tracer flowrate in the channel
$\phi'$ = tracer leak discharge rate out of the channel
$\overline{\phantom{x}}$ = time average of a fluctuation
$+$ = nondimensionalization according to dynamic parameters
$++$ = nondimensionalization according to mass transfer parameters
$\langle\,\rangle$ = spatial average of a time average value

## Literature Cited

Aïsa, L., "Absorption à une Interface Gaz-Liquide en Écoulement Stratifié ou Ondulé," PhD Thesis, Institut National Polytechnique de Toulouse (1978).

Aïsa, L., B. Caussade, J. George, and L. Masbernat, "Echanges de Gaz Dissous en Écoulements Stratifiés de Gaz et de Liquide, *Int. J. of H.M. Transfer,* **24**(6), 1005 (1981).

Back, D. D., and M. J. McCready, "Effect of Small Wavelength Waves on Gas Transfer across the Ocean Surface," *J. Geophys. Res.,* C5, **93,** 5143 (1988).

Baleix, A., "Contribution à l'Étude de l'Influence du Nombre de Schmidt dans le Phénomène d'Absorption," Thèse de 3e Cycle, Institut National Polytechnique de Toulouse (1984).

Baird, M. H. I., and J. F. Davidson, "Annular Jets: II. Gas Absorption, "*Chem. Eng. Sci.,***17,** 473 (1962).

Benson, B. B., and D. Krause, Jr., "Empirical Laws for Dilute Aqueous Solutions of Nonpolar gases," *J. Chem. Phys.,* **64,** 689 (1976).

Boerboom, A. J. H., and G. Kleyn, "Diffusion Coefficients of Nobles Gases in Water" *J. Chem. Phys.,* **50,** 1086 (1969).

Broecker, H. C., J. Petermann, W. Siems, "The Influence of Wind on $CO_2$ Exchange in a Wind-Wave Tunnel, Including the Effects of Monolayers," *J. Marine Res.,* **36,** 595 (1978).

Caussade, B., J. George, D. Marodon, and L. Masbernat, "Mathematical Modelling of Stratified Two-Phase Flow," *Symp. on Refined Modelling of Flows,* Presses de l'Ecole des Ponts et Chaussées, Paris (1982).

Coantic, M., "A Model of Gas Transfer across Air-Water Interfaces with Capillary Waves," *J. Geophys. Res.,* **91,** 3925 (1986).

Danckwerts, P. V., "Significance of Liquid-Film Coefficients in Gas Absorption," *Ind. Eng. Chem.,* **43,** 1460 (1951).

Davies, J. T., A. A. Kilner, G. A. Ratcliff, "The Effect of Diffusivities and Surface Films on Rates of Gas Absorption," *Chem. Eng. Sci,* **19,** 583 (1964).

*Encyclopedie des Gaz de l'Air Liquide,* Elsevier Publishing (1976).

Fabre, J., L. Masbernat and C. Suzanne, "New Results on the Structure of Stratified Gas-Liquid Flow," NATO Advanced Research Workshop on Two Phase Flows and Heat Transfer, Spitzingsee, West Germany (1982).

Ferrell R. T., and D. M. Himmelblau, "Diffusion Coefficients of Hydrogen and Helium in Water," *AIChE J.* **13,** 702 (1967).

Fernandez Flores, R., "Etude des Interactions Dynamiques en Écoulement Diphasique Stratifié," PhD Thesis, Toulouse (1984).

Fortescue, G. E., and J. R. A. Pearson, "On Gas Absorption into a Turbulent Liquid," *Chem. Eng. Sci.,* **22,** 1163 (1967).

Gastel van, K., P. A. E. M. Janssen and G. J. Komen, "On Phase Velocity and Growth Rate of Wind-Induced Gravity-Capillary Waves," *J. of Fluid Mechanics,* **161,** 199 (1985).

George, J., "Etude de l'Absorption d'un Gaz peu Soluble à une Interface Gaz-Liquide," Rapport Interne 336 E.M.E.-I.M.F., Toulouse (1987).

Hasse L., and P. L. Liss, "Gas Exchange Across the Air Sea Interface," *Symp. on Capillary Waves and Gas Exchange,"* Hambourg, 147 (1980).

Higbie, R., "The Rate of Absorption of a Pure Gas into a Still Liquid during Short Periods of Exposure," *Trans. AIChE,* **35,** 365 (1935).

*International Critical Tables,* Vol. 3, 257, McGraw Hill, New York (1928).

Jähne, B., K. O. Munnich, R. Bosinger, A. Dutzi, H. Huber, and P. Libner, "On the parameters Influencing Air-Water Gas Exchange," *J. Geophys. Res.,* **C2**(92), 1937 (1987).

Jähne, B., K. O. Munnich and U. Siegenthaler, "Measurements of Gas Exchange and Momentum Transfer in a Circular Wind Wave Tunnel," Tellus 31, 321 (1979).

Kitaïgorodskii, S. A., "On the Fluid Dynamical Theory of Turbulent Gas Transfer across an Air Sea Interface in the Presence of Breaking Waves," *J. of Physical Oceanography,* **14,** 960 (1984).

Kitaïgorodskii, S. A., M. A. Donelan, J. L. Lumley, and E. A. Terray "Wave-Turbulence Interactions in the Upper Ocean: II," *J. Physical Oceanography,* **13,** 1988 (1983).

Krieger, I. M., G. W. Mulholland, C. S. Dickey, "Diffusion Coefficients for Gases in Liquids from the Rates of Solution of Small Gas Bubbles," *J. Physical Chemistry,* **71,** 1123 (1967).

Lamont, J. C., and D. S. Scott, "An Eddy Cell Model of Mass Transfer into the Surface of a Turbulent Liquid" *AIChE J.,* **16,** 513 (1970).

Ledwell, J. J., "The Variation of the Gas Transfer Coefficient with Molecular Diffusivity," *Gas Transfer at Water Surfaces,* Brutsaert and Jirka, eds. 293, Reidel Publishing (1984).

Levich, V. G., *Physico-Chemical Hydrodynamics,* Prentice Hall, Englewood Cliffs, NJ (1962).

Liss, P. S., "Processes of Gas Exchange across an Air Water Interface," *Deep-Sea Res.,* **20,** 221 (1973).

McCready, M. J., and T. J. Hanratty, "A Comparison of Turbulent Mass Transfer at Gas-Liquid and Solid-Liquid Interfaces, " *Gas Transfer at Water Surface, Brutsaert and Jirka, eds., Reidel Publishing (1984).*

Maharajh, D. M., and J. Walkley, *Can. J. Chem. Eng.,* **51,** 944 (1973).

Marodon, D., "Turbulence en Ecoulement d'Eau Cisaillé par le Vent," PhD Thesis, Toulouse (1983).

Mattingly, G. E., "Experimental Study of Wind Effects on Reaeration," *J. of Hydrualics Division, ASCE,* Hy 3, **103,** 311 (1977).

Mazarei, A. F., and O. C. Sandall, "Diffusion Coefficients for Helium, Hydrogen and Carbon dioxide in Water at 25°C," *AIChE J.,* **26,** 15 (1980).

Merlivat, L., and L. Memery, "Exchange across an Air-Water Interface: Experimental Results and Modelling of Bubble Contribution to Transfer," *J. Geophys. Res.,* **88,** 707 (1983).

Moussa, M., "Turbulence et Circulation Générées par le Vent dans les Systèmes Aquatiques peu Profonds: Application au lac de Tunis, PhD Thesis, I.N.P., Toulouse (1986).

Sivakumar, M., "Reaeration and Wind Induced Turbulence Shear in a Contained Water Body," *Gas Transfer at Water Surfaces,* Brutsaert and Jirka, eds., Reidel Publishing (1984).

Souyri, A., "Turbulence sous les Vagues de Vent en Écoulement Isotherme ou Thermiquement Stratifié," PhD Thesis, I.N.P., Toulouse (1986).

Stewart, W. E., "Forced Convection: IV. Asymptotic Forms for Laminar and Turbulent Transfer Rates," *AIChE J.,* **33,** 2008 (1987).

Suzanne, C., "Structure de l'Ecoulement Stratifié de Gaz et de Liquide en Canal Rectangulaire," PhD Thesis, I.N.P., Toulouse (1985).

Thomas, W. J., and M. J. Adams, "Measurements of the Diffusion Coefficients of Carbon Dioxide and Nitrous Oxide in Water and Aqueous Solutions of Glyceral," *Trans. Far. Soc.,* **61,** 668 (1965).

Tsacoyannis, Y., "Etude de l'Absorption d'un Gaz par un Liquide en Écoulement Turbulent Stratifié," PhD Thesis. U.P.S., Toulouse (1976).

Unver, A. A., and D. M. Himmelblau, "Diffusion Coefficients of $CO_2$, $C_2H_4$, $C_3H_6$ and $C_4H_8$ in Water from 6°C to 65°C," *J. of Chem. Eng. and Data,* **9,** 428 (1964).

Vivian, J. E., and C. J. King "Diffusivities of Slightly Soluble Gases in Water," *AIChE J.,* **10,** 220 (1967).

Weiss, R. F., "Solubility of Helium and Neon in Water and Sea Water," *J. Chem. Eng. Data,* **16,** 235 (1971).

Whitman, W. G., "Preliminary Experimental Confirmation of the Two-Film Theory of Gas Absorption," *Chem. Metall. Eng.,* **29,** 146 (1923).

Wise, D. L., and G. Houghton, "The Diffusion Coefficients of Ten Slightly Soluble Gases in Water at 10–60°C," *Chem. Eng. Sci.,* **21,** 999 (1966).

Yaglom, A. M., and B. A. Kader, "Heat and Mass Transfer between a Rough Wall and Turbulent Fluid Flow at High Reynolds and Peclet Numbers," *J. of Fluid Mechanics,* **62,** 601 (1974).

*Manuscript received May 11, 1989, and revision received Dec. 8, 1989.*